Available online at www.sciencedirect.com
ScienceDirect
Applied Surface Science 253 (2007) 8398–8403
applied surface science
www.elsevier.com/locate/apsusc

Structure and mechanical properties of ceramic coatings fabricated by plasma electrolytic oxidation on aluminized steel

Zhenqiang Wu [a,b], Yuan Xia [a,*], Guang Li [a], Fangtao Xu [a,b]

[a] Institute of Mechanics, Chinese Academy of Science, Beijing 100080, China
[b] Graduate School of the Chinese Academy of Sciences, Beijing 100049, China

Received 6 January 2007; received in revised form 3 April 2007; accepted 3 April 2007
Available online 8 April 2007

Abstract

Ceramic coatings were formed by plasma electrolytic oxidation (PEO) on aluminized steel. Characteristics of the average anodic voltages versus treatment time were observed during the PEO process. The micrographs, compositions and mechanical properties of ceramic coatings were investigated. The results show that the anodic voltage profile for processing of aluminized steel is similar to that for processing bulk Al alloy during early PEO stages and that the thickness of ceramic coating increases approximately linearly with the Al layer consumption. Once the Al layer is completely transformed, the FeAl intermetallic layer begins to participate in the PEO process. At this point, the anodic voltage of aluminized steel descends, and the thickness of ceramic coating grows more slowly. At the same time, some micro-cracks are observed at the Al_2O_3/FeAl interface. The final ceramic coating mainly consists of γ-Al_2O_3, mullite, and α-Al_2O_3 phases. PEO ceramic coatings have excellent elastic recovery and high load supporting performance. Nanohardness of ceramic coating reaches about 19.6 GPa.

Keywords: Hot-dip aluminum; Plasma electrolytic oxidation; Ceramic coatings; Steel substrate

1. Introduction

Plasma electrolytic oxidation (PEO) is a new technique for fabricating metallurgically bonded ceramic coatings on light metals such as Al, Mg, Ti, etc. and their alloys. It is generally considered to be a cost-effective and environmentally friendly surface engineering technique and can be used in many application fields such as automotive, aerospace, medicine, etc. [1–3]. It has previously been shown that the PEO coatings on aluminum substrates are mainly composed of α-Al_2O_3 and γ-Al_2O_3, and have a maximum hardness of about 2535 Hv [4]. The anti-wear, anti-corrosion and heat-resisting performance of metal substrates can be improved substantially by the application of PEO coatings [5,6]. As we know, steel is used widely in industry but its performances in bearing wear and corrosion are not optimal. Recently, some researchers report that the PEO techniques can be applied to steel, with good adhesion achieved between the steel and ceramic coating [7–16].

There are two distinct ways of plasma electrolysis techniques for making ceramic coatings on steel surface from the viewpoint of electrodes. One is cathodic micro-arc electrodeposition where the steel is used as the cathode and cathodic discharges occur during treatment. In 2003, Yang [7] prepared yttrium stabilized zirconia (YSZ) coatings on FeCrAl alloy using this method. Studies of this method are limited, but it appears that the coating content comes mainly from the electrolyte. The other technique exploits an anodic barrier layer on the substrate. Since the steel material has low passivation in PEO electrolytes, the anodic voltage does not increase with treatment time, and the anodic discharge cannot occur. In order to enhance the passivation of steel, an anodic barrier layer is first deposited on substrate by a separate process. For example, in 1987, Saakiyan et al. [8] formed alumina coating on steel by arc-sprayed aluminum, followed by PEO processing. In 1998, Tan et al. [9] deposited glassy silicates and amorphous zinc oxides coatings on galvanized steel by PEO technique.

Al layers can be fabricated on steel to act as anodic barrier layers using many conventional surface techniques, such as arc spraying [10,11], hot-dip aluminum (HDA) [12–15], and plasma sputtering aluminum [16]. In this work, the composite

* Corresponding author. Tel.: +86 10 62554190; fax: +86 10 62561284.
E-mail address: xia@imech.ac.cn (Y. Xia).

0169-4332/$ – see front matter © 2007 Elsevier B.V. All rights reserved.
doi:10.1016/j.apsusc.2007.04.007

ceramic coatings were prepared by HDA and PEO combined technology. In addition, microstructres, growth regularity and elemental distribution of PEO coatings are discussed.

2. Experimental procedure

Rectangular samples of Q235 steel (25 mm × 20 mm), having the nominal composition (wt.%) (0.14–0.22 Cu, 0.30–0.65 Mn, 0.3 Si, 0.045 P, Fe balance) were used as substrates. The material for hot dipping was the industrial pure aluminum (99.99% purity). The thickness of the resulting Al layer was 30–50 μm, with an FeAl layer about 60 μm thick. Ceramic coatings were prepared using a 5 kW DC bipolar pulse power with the frequency of 50 Hz. An alkali-silicate solution (16 g/l Na_2SiO_3 and 2 g/l NaOH) was used as the electrolyte. The constant current density on specimen's surface was maintained at 4 A/dm^2 during the PEO process, and the ratio of anodic current to cathodic current was 1. The temperature of the electrolyte was controlled below 30 °C by employing a cooling system. The anodic voltage variation was recorded by the signal detection and the controlling system.

Cross-sectional micrographs were observed using an XJP-6A metallographical microscope and the thickness of coatings was determined by microscope. Phase compositions of coating were analyzed with an X'Pert Pro MPD X-ray diffractometer (XRD) working on Cu Kα radiation. The X-ray generator settings were 40 kV and 30 mA. Surface morphologies and elemental compositions of coatings were investigated using a FEI Quanta 200 FEG scanning electron microscopy (SEM) with energy dispersive spectroscopy (EDS). For SEM and EDS test, thin carbon films were sprayed on the samples to provide a conductive surface. Microscale mechanical properties were evaluated using a MicroMaterials Nano Indenter XP system, with the depth of nanoindentation tests set to 500 nm.

3. Results and discussion

3.1. The average anodic voltage–time response

Fig. 1 shows how the average anodic voltages of HDA and pure aluminum vary during PEO treatment. The average voltage is about 90 V for pure aluminum and 70–80 V for hop-dip aluminum. Though the average voltage is relatively low, the peak voltage of every pulse is at 200–500 V, which is high enough to generate the electrical breakdown of the ceramic coating and discharging sparks are observed at the surface of sample during treatment process. Literature [3,17] indicates that the average anodic voltage of Al alloy increases with the time, which is divided into three or four stages according to the increasing rate of voltage. However, the decreasing anodic voltage of HDA at the end of treatment time is different from that of Al alloy. In our work, four stages can be found in the PEO process of the HDA sample. The first stage corresponds to conventional anodic oxidation, with rapidly increasing voltage. It is found that the anodic voltage reaches 70 V in a few minutes and many gas bubbles are generated instantly at sample surface. The PEO process enters the second stage several minutes later, which

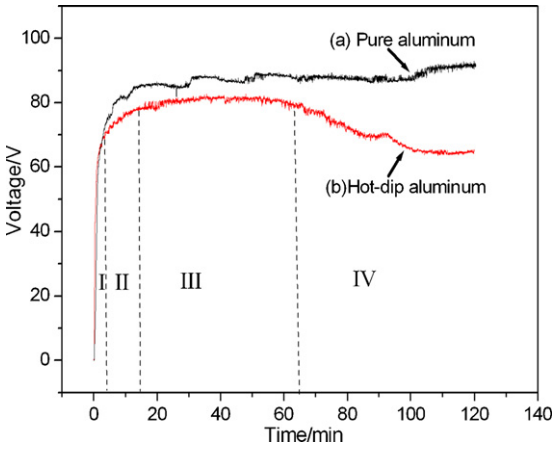

Fig. 1. The average anodic voltage vs. time response.

comprises spark oxidation and the transition process from spark oxidation to plasma electrolytic oxidation. Simultaneously, there are many small sparks moving quickly at the sample surface. The color of sparks changes from bright white to orange. The third stage is the process of plasma electrolytic oxidation, which is the main process of fabricating the ceramic coatings. The anodic voltage increases slowly during this period. I–III stages coincide with the PEO stages of Al alloys. In contrast with the sample of pure aluminum, the anodic voltage of the HDA sample drops in the last stage (as showed in curve (b) of Fig. 1) and only a few discharges can be observed at the surface.

3.2. Surface morphologies of ceramic coatings

Fig. 2 shows surface morphologies of ceramic coatings with different treatment time. A thin passivating film is formed at the beginning of PEO process (1–2 min) with many small pores distributing uniformly on the surface with sizes of less than 1 μm. As shown in Fig. 2a–f, some crater-alike structures appear which consist of the oxides, discharge channels and floccules around crater. Some studies have indicated that the instantaneous temperature in discharge channels is of the order of several thousands of degrees [2,11]. Molten oxides are produced in the channels and they react transiently with electrolyte. The oxides are solidified rapidly and some floccules are also deposited around the discharge zones. The thickness of the ceramic coating grows with the PEO treatment time, which needs progressively more energy for the disruptive discharges of coating. At the same time, the number of pores decreases and the size of pores increases. Some cracks form during the solidification as of the molten oxides and emerge from the crater holes. The diameters of some pores reach 30 μm in the final stages of PEO processing, which are larger than those of normal, bulk Al or Mg alloy PEO coatings.

3.3. Cross-sectional micrographs and element distribution

Fig. 3 shows the variations of cross-sectional micrographs of HDA/PEO coatings. These coatings are multilayer structures and comprise three layers from substrate to surface: a FeAl

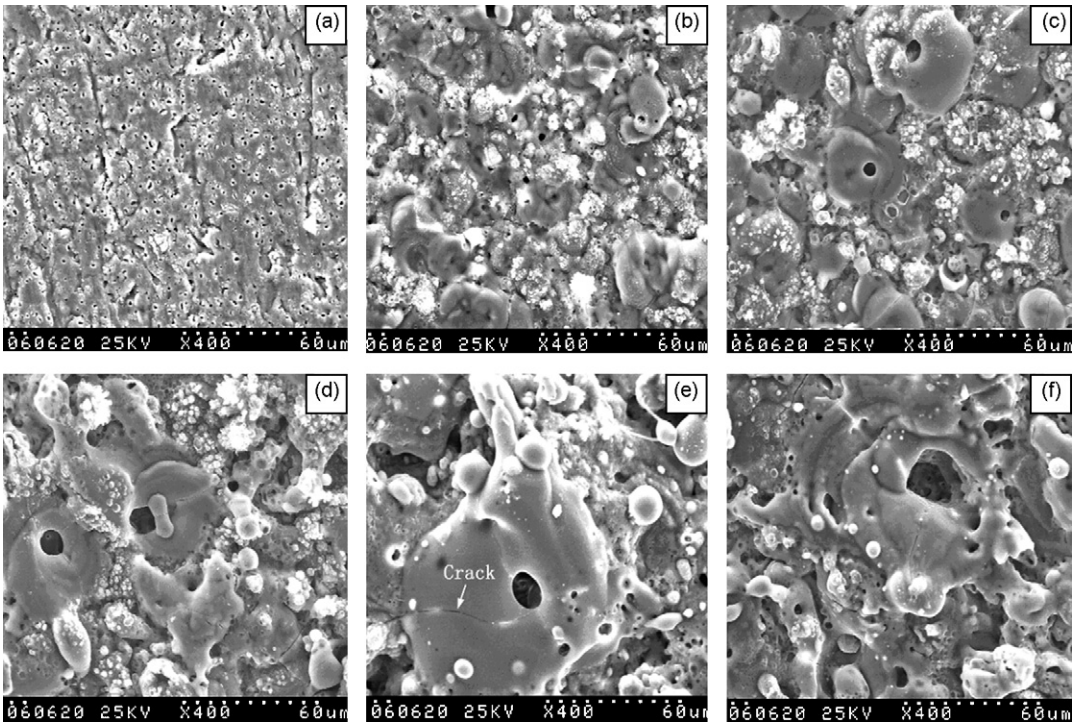

Fig. 2. Surface morphologies of ceramic coatings on aluminized steel (a) 1 min, (b) 30 min, (c) 60 min, (d) 90 min, (e) 105 min (f) 120 min.

layer, an Al layer and an Al_2O_3 layer. The FeAl layer is formed by the intermetallic reaction of Fe and Al elements and mutual diffusion during the hot-dip process. The ceramic coating at the surface is loose, while the ceramic coating near Al layer is relatively dense. It also can be seen that there is a transition layer of average thickness 5–10 μm between the FeAl and the Al layer. However, there is no transition layer but an abrupt interface between the Al layer and the ceramic layer. Fig. 3b shows that most parts of Al layer have already been oxidized and some discrete Al particles exist near the Al_2O_3/FeAl interface. When the whole Al layer is oxidized into ceramic coating, the discharges of the PEO process do not cease altogether because the FeAl layer becomes involved in the PEO process. Some cracks are observed at the Al_2O_3/FeAl interface, as shown in Fig. 3c. The cause of these cracks is the brittleness of the FeAl layer and the high cooling rate at discharge channels. It can be concluded that the thin Al layer or Al particles have good plasticity and can improve the interface toughness of the ceramic coating.

HDA/PEO coating typically has a tri-layered structure when treated by PEO for 75 min, and the elemental distribution along the cross-section is shown in Fig. 4. There is a certain content of Si in the external ceramic layer, but Si content is lower in the internal ceramic layer, Al layer, FeAl layer or substrate. Al content fluctuates also within ceramic coating. During the discharge process of PEO, the molten oxides are ejected from the discharge hole and are solidified instantly which will have much Al content, while floccules are sintered around crater and possess a great deal of Si. Moreover, the O content distributes almost uniformly within ceramic coatings. Fe content increases from the surface towards the steel substrate and there is a gradient of Fe at the Al/FeAl interface.

As shown in Fig. 4, A and B are the points of external and internal parts of PEO ceramic coating, respectively. The element content of points A and B of ceramic coating is shown in Table 1. Ceramic coatings are composed of Al, Si, and O and a little Fe. Al comes from the hot-dip aluminum layer, while Si and O come from the silicate electrolyte. The FeAl layer did not

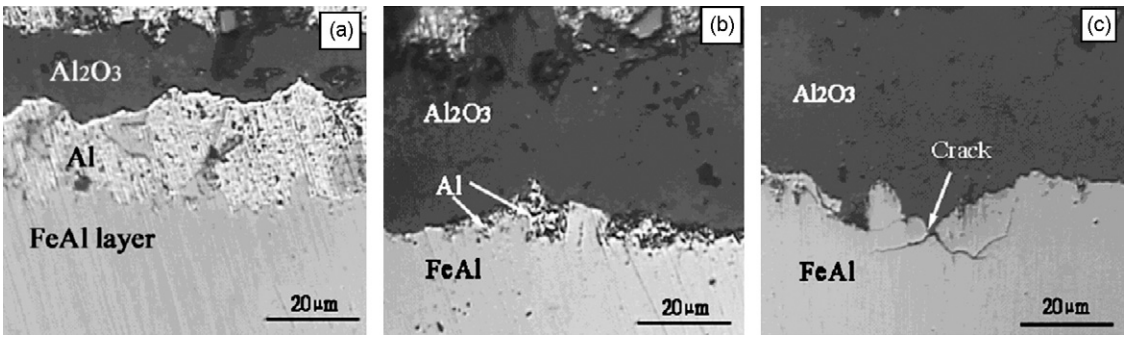

Fig. 3. Cross-sectional micrographs of coatings (a) 30 min, (b) 90 min, (c) 120 min.

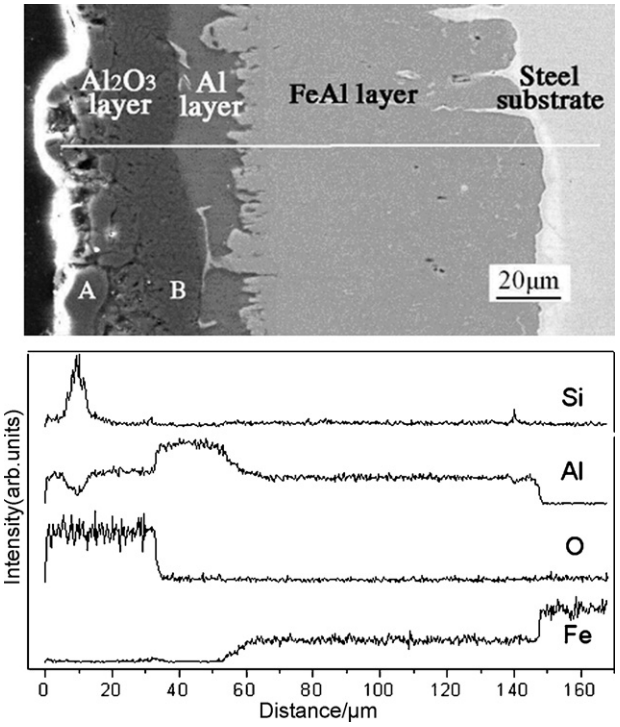

Fig. 4. Element distribution along the coating profile.

participate in the PEO process at that time because there was a thin Al layer between Al_2O_3 layer and FeAl layer. Thus, the little Fe content of points A and B is perhaps just due to the impurity of hot-dip aluminum or Fe diffusing into molten aluminum during hot dipping. Through comparing values of the different chemical compositions at points A and B, the O and Al elements are almost same in both outside and inside of coating. The atomic percent of Si at the surface is 3.5%, while it is only 1.5% inside the ceramic coating. The atomic percent of Fe of ceramic layer is less than 0.5%.

When the Al layer is oxidized completely into ceramic coating, the FeAl/Al interface or FeAl layer participates in PEO process. So Fe also undergoes melting and co-deposition with the molten alumina and there is more Fe within ceramic layer. For instance, Fe content of point P which locates at the internal part of a ceramic coating treated by PEO for 120 min increases up to about 1.0%.

3.4. Coating thickness

Fig. 5 shows the thickness of the residual Al layer and ceramic coating, where δ_{Al} is the thickness of Al layer before PEO treatment. During the initial stage, the ceramic coating

Table 1
Chemical compositions (at.%) of external and internal parts of coating as shown in Fig. 44

Points	O	Al	Si	Fe
External A	53	43	3.5	0.4
Internal B	53	45	1.5	0.3
Point P	54	44	1.1	1.0

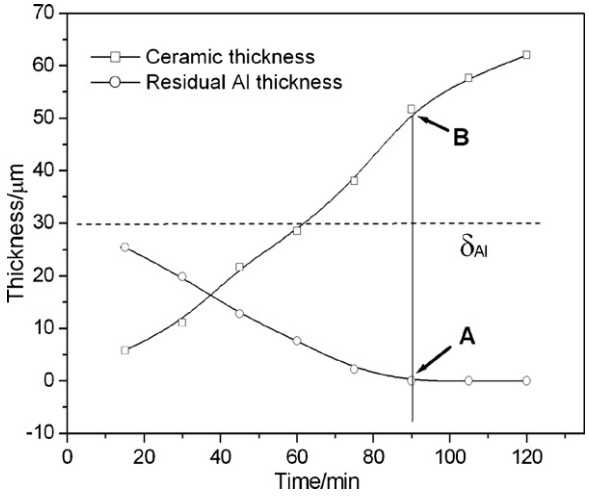

Fig. 5. The thickness of residual Al thickness and ceramic coating.

thickness increases linearly and Al layer is oxidized linearly. The growth rate of ceramic coatings is larger than the oxidized rate of Al layer, so the PEO coating grows both inwards and outwards. Point A in Fig. 5 corresponds to the Al layer being completely transformed into ceramic coating. Point B in Fig. 5 is where the FeAl begins to participate in PEO process. However, the thickness of ceramic coating grows slowly between 90 and 120 min.

3.5. Phase structure

XRD patterns for the phase structures of PEO coatings are given in Fig. 6. The strong Al peaks in XRD patterns come mainly from Al layer. When treated only for 30 min, the ceramic coating is very thin and there are many pores and discharge holes within coatings, so X-rays can penetrate through the ceramic coating and reach the Al layer. When the HDA sample has been treated for 105 min, the diffraction intensity of aluminum peak is very low. PEO coatings contain mainly γ-Al_2O_3 and mullite phases at different treatment time, yet the α-Al_2O_3 phase appears only when PEO process is

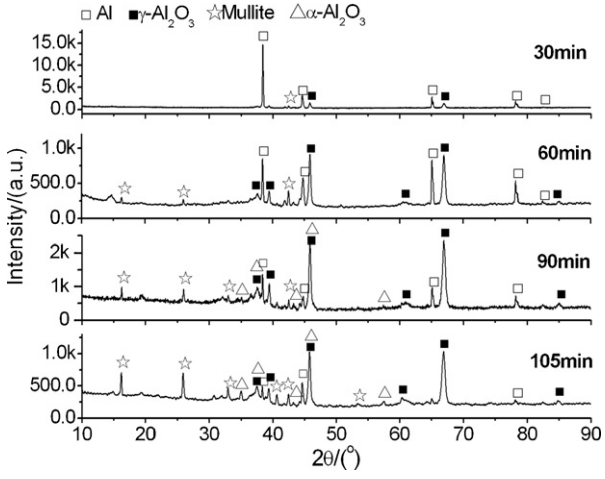

Fig. 6. XRD analysis of ceramic coating at different PEO treatment time.

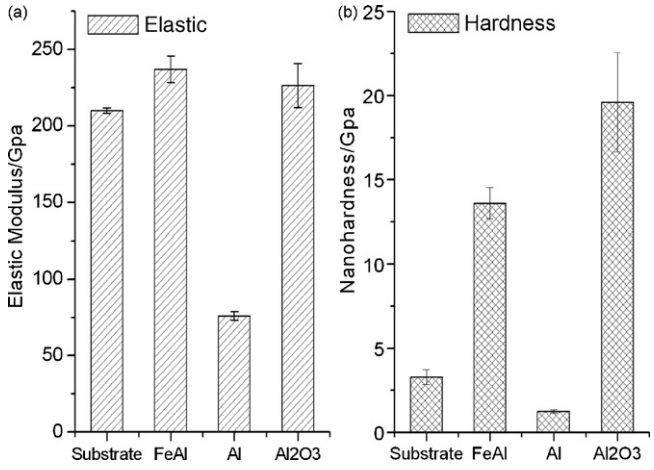

Fig. 7. Micro-mechanical properties of HDA/PEO coating (a) elastic modulus, (b) nanohardness.

carried out for a long time. The instantaneous temperature in discharge zone can reach several thousands degrees which can cause the Al_2O_3 melting. When contacting with the electrolyte, molten oxides are solidified to form γ-Al_2O_3, α-Al_2O_3 or other phases. The higher cooling rate at coating/electrolyte interface favors the formation of the γ-Al_2O_3. On the contrary, the α-Al_2O_3 phase is easily formed in the internal layer with a lower cooling rate [2]. In particular, more α-Al_2O_3 phases are found in thicker coatings at the final stage of PEO process. Furthermore, parts of γ-Al_2O_3 phases can also be transformed into α-Al_2O_3 during spark or microarc discharge. Mullite phase is the result of the reaction between the molten alumina and cations which come from the sodium silicate electrolyte.

3.6. Mechanical property

Fig. 7 shows nanohardness and elastic modulus of HDA/PEO coating. It indicates that elastic moduli of Al_2O_3 layers, FeAl layers and substrates are about 200 GPa and that of the Al layer is only 70 GPa. However, the hardness of steel substrate is increased greatly by the PEO process. The maximum hardness of ceramic coating is over 19 GPa, which is larger about 15 times than that of Al layer. Fig. 8 illustrates the load-displacement curves of indentation. During the process of indentation, the steel substrate and Al layer undergo chiefly plastic deformation. For instance, the elastic recovery of Al layer is about 34 nm after unloading, which is just 6.5% of the whole displacement. On the contrary, Al_2O_3 has strong supporting performance and excellent elastic recovery. Though the elastic modulus of the Al_2O_3 layer is lower than that of FeAl layer, the elastic recovery of Al_2O_3 layer is larger than that of FeAl layer. The elastic modulus of PEO coating is lessened by γ-Al_2O_3, amorphous phases and some pores. Some corundum (α-Al_2O_3) within coating can increase the hardness of ceramic coatings.

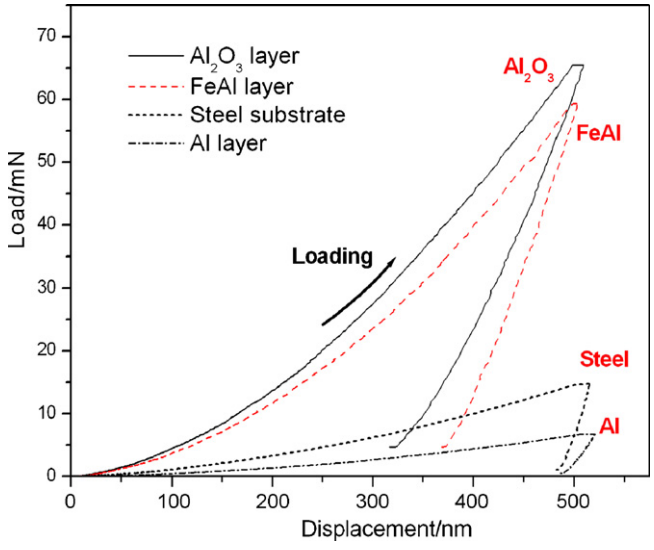

Fig. 8. Load–displacement curves of nanoindentation.

4. Conclusions

Affected by FeAl layer, the average anodic voltage of HDA sample shows a different variation characteristic. It varies in a pattern as similarly as that of Al alloys during I–III stages, but it descends at last stage. During the PEO treatment of HDA sample, the Al layer becomes thin and is transformed into ceramic coating. When the Al layer is completely consumed, the FeAl layer begins to participate in the PEO process. In this stage, the ceramic coating grows more slowly and some micro-cracks are observed at the Al_2O_3/FeAl interface. Ceramic coating is mainly composed of Al, Si and O with a little Fe. In comparison to the steel substrate, the PEO ceramic coating has high hardness, excellent elastic recovery and strong supporting performance.

Acknowledgements

The authors would like to thank the financial supports of the National Nature Science Foundation of China (No: 10572141) and the 19th Opening Project of State Key Laboratory of Nonlinear Mechanics (LNM), Institute of Mechanics, Chinese Academy of Sciences. The authors with to thank Mr. J.A. Curran of University of Cambridge for advises of revising this paper.

References

[1] A.L. Yerokhin, X. Nie, A. Leyland, A. Matthews, Surf. Coat. Technol. 122 (1999) 73–93.
[2] W.B. Xue, Z.W. Deng, R.Y. Chen, T.H. Zhang, Thin Solid Films 372 (2000) 114–117.
[3] Y.J. Guan, Y. Xia, Trans. Nonferrous Met. Soc. 16 (2006) 1097–1102, China.
[4] H.H. Wu, J.B. Wang, B.Y. Long, B.H. Long, Z.S. Jin, N.D. Wang, F.R. Yu, D.M. Bi, Appl. Surf. Sci. 252 (2005) 1545–1552.
[5] X. Nie, E.I. Meleties, J.C. Jiang, A. Leyland, A.L. Yerokhin, A. Matthews, Surf. Coat. Technol. 142–144 (2002) 1129–1136.
[6] S.G. Xin, L.X. Song, R.G. Zhao, X.F. Hu, Mat. Chem. Phys. 97 (2006) 132–136.
[7] X.Z. Yang, Y.D. He, D.R. Wang, W. Gao, Chin. Sci. Bull. 48 (8) (2003) 746–750.
[8] L.S. Saakiyan, A.V. Efremov, A.V. Epelfeld, E.F. Korytnyi, V.A. Popov, Fiz. Khim. Mekh. Mater. 23 (6) (1987) 88–90.

[9] T.R. Tan, J.R. Cheng, J.H. Wang, J.G. Duh, H.C. Shih, Surf. Coat. Technol. 110 (1998) 194–199.
[10] V.B. Lazarev, V.P. Sanygin, A.M. Kvardakov, L.S. Saakiyan, A.P. Efremov, A.V. Kutsev, Neorg. Mater. 27 (4) (1991) 741–746.
[11] W.C. Gu, D.J. Shen, Y.L. Wang, G.L. Chen, W.R. Feng, G.L. Zhang, S.H. Fan, C.Z. Liu, S.Z. Yang, Appl. Surf. Sci. 252 (2006) 2927–2932.
[12] S.X. Yu, Y. Xia, Y.J. Guan, Trans. Nonferrous Met. Soc. 14 (Suppl. 2) (2004) 310–314, China.
[13] W.C. Gu, G.H. Lv, H. Chen, G.L. Chen, W.R. Feng, G.L. Zhang, S.Z. Yang, J. Alloys Compd. 430 (2007) 308–312.
[14] S.Y. Xie, C.Z. Wang, B.D. Kou, X.K. Su, J. Ma, Light Alloy Fabric. Technol. 31 (9) (2003) 35–38, In Chinese.
[15] Z.S. Yang, J.F. Jia, J. Tian, D.Y. He, J. Inorg. Mater. 19 (6) (2004) 1446–1450, In Chinese.
[16] A.P. Efremov, Prot. Met. 25 (2) (1989) 176–180.
[17] L. Wang, X. Nie, Thin Solid Films 494 (1–2) (2006) 211–218.